Pharmaceutical Analytical Chemistry: Open Access

Naijing et al., Pharm Anal Chem Open Access 2015, 1:1
DOI: 10.4172/2471-2698.1000108

Research Article Open Access

Brain Metabolomics Study on the Protective Effects of Ginsenosides Rg1 and Rb1 in an Alzheimer's Disease Mouse Model

Naijing Li[1*], Ling Zhou[2], Wei Li[2], Ying Liu[2], Xiu Gu[1], Yang Peng[1] and Ping He[1]

[1]*Department of Gerontology, The Shengjing affiliated Hospital, China Medical University, Shenyang 110004, Liaoning, China*
[2]*College of Pharmacy, Shenyang Pharmaceutical University, Shenyang 110004, Liaoning, China*

Abstract

Alzheimer's disease (AD) is a serious neurodegenerative disease in aging populations with no effective method for the diagnosis or for the treatment. Although some physiological and pathological functional parameters have been studied, little knowledge about the changes of small metabolites in biofluids has been reported, which may result in poor diagnosis and treatment for AD. Ginsenoside Rg1 and Rb1, the pharmacologically active ingredients of ginseng, were known to have anti-AD effects, while, their mechanism remain unclear completely. This study was designed to explore globally metabolomic character of AD induced by Aβ1-42 in brain and the holistic efficacy of ginsenoside Rg1 (GRg1) and ginsenoside Rb1 (GRb1) on AD. Morris water maze was performed to examine the behavioral changes in mice. Global metabolic profiling with UPLC/MS (ultra-high-performance liquid chromatography-mass spectrometry) and principal component analysis (PCA) were performed to discover differentiating metabolites. A total of 9 potential biomarkers were identified that were associated with the metabolism of lecithin, purine, and sphingolipids in AD mice. The peak intensities of lysophosphatidylcholine, dihydrosphingosine, hexadecasphinganine, phytosphingosine were lower, while that of hypoxanthine and ceremide were higher, in AD than in control mice. GRg1 and GRb1 treatment affected lecithin and sphingolipid pathways, while not purine metabolism. These results provide the first evidence of a link between metabolite imbalance and AD, and reveal a molecular basis for the therapeutic benefits of ginsenosides in AD treatment.

Keywords: Alzheimer's disease; Brain; UPLC/MS; Ginsenoside Rg1; Ginsenoside Rb1

Introduction

Alzheimer's disease (AD) is among the most debilitating neurodegenerative diseases in aging populations, and is characterized by progressive memory loss and the impairment of behavioral, language, and visuospatial skills [1]. AD affects millions of people both in developed and developing countries and has become a major medical and social problem all over the world [2], while there is no effective method for its treatment to date. Thus, there is a critical need to identify agents that can prevent AD progression.

Ginseng, a key agent in traditional Chinese medicine, is widely used to improve memory and delay senescence. Currently, many in vivo and in vitro studies have shown its beneficial effects in aging, central nervous system (CNS) disorders, and neurodegenerative diseases, such as AD [3,4]. Ginsenosides Rg1 (GRg1) and Rb1 (GRb1) as the main pharmacologically active ingredients of ginseng have been proved in their effectiveness in AD prevention and treatment [5,6]. In addition, previous studies have demonstrated that they exert its effects on multiple sites of action like Regulation of neurite outgrowth [7], inhibition of Neuroinflammation [8], reducing the level of Aβ [9] and so on. To date, previous studies have mainly focused on the biochemical and pathological changes that occur in AD, while few studies have examined changes in metabolite profiles upon treatment with GRg1 and GRb1, or examined how these agents affect metabolism.

Metabolomics, based on the comprehensive and simultaneous analyses of multiple metabolites in biological samples, demonstrates a great potential in health survey for the study of disease pathology, discovery of biomarkers and drug development since metabolites represent the end point of biological reactions, reflecting well the interactions between genes, proteins and the environment [10]. Thereby, several metabolomics studies have been performed in the last years for the investigation of AD [11]. Most of these studies have been performed in biofluids because of the difficult availability of human brain tissue. Thus, only a few preliminary studies have been previously reported in this subject [12-14], demonstrating the potential of this approach.

Rodents injected with $A\beta_{1-42}$ have been used as a classical AD animal model for drug screening [15]. The administration of Aβ peptide induces memory loss [16], and acute injection of $A\beta_{1-42}$ into the brain leads to dysfunction followed by neurodegeneration and also impairs learning and memory in a process similar to that observed in AD [17,18].

In this study, a metabolomics platform based on complementary analysis by reversed-phase ultra-high performance liquid chromatography-mass spectrometry (UPLC-MS) was used to investigate metabolic perturbations in the brain of AD mice and to investigate protective effects of GRg1 and GRb1. A principal component analysis (PCA) was carried out to estimate the changes in brain metabolite levels and identify highly sensitive and specific biomarkers for AD. All these studies would provide a theory and practice basis for the early diagnosis and treatment of AD.

***Corresponding authors:** Naijing Li, The Shengjing affiliated Hospital, China Medical University, Shenyang, PR China, Tel: +86-24 23894342; Fax: +86-24 83956720; E-mail: lnjlw2003@163.com

Received November 17, 2015; **Accepted** November 24, 2015; **Published** November 26, 2015

Citation: Naijing Li, Zhou L, Li W, Liu Y, Gu X, et al. (2015) Brain Metabolomics Study on the Protective Effects of Ginsenosides Rg1 and Rb1 in an Alzheimer's Disease Mouse Model. Pharm Anal Chem Open Access 1: 108. doi:10.4172/2471-2698.1000108

Materials and Methods

Reagents

GRg1 and GRb1 (purity ≥ 98%) were purchased from Shanghai Yuanye Bio-Technology Co. (Shanghai, China). High performance LC grade methanol and acetonitrile were purchased from Fisher Scientific (Bridgewater, NJ, USA). Water was purified by redistillation and filtration through a 0.22 μm membrane. $A\beta_{1-42}$ peptide (Sigma, St. Louis, MO, USA) and analytical grade formic acid were from the Department of Pharmaceutics, Shenyang Pharmaceutical University (Shenyang, China).

Animals

Male 12 week old Kun Ming mice weighing 18-22 g were purchased from the Central Animal House of Shenyang Pharmaceutical University (Shenyang, China). Mice were housed five per cage under controlled conditions (temperature 20°C ± 2°C, relative humidity 55% ± 10%, 12:12 h light/dark cycle with lights on from 07:00 to 19:00 h) with free access to food and water. Experiments were conducted in accordance with the regulations for animal experimentation issued by the State Committee of Science and Technology of China.

$A\beta_{1-42}$ protein injection and drug administration

Mice were randomly divided into 9 groups (with 10 animals each): normal (no lesion, saline-treated), control (saline-lesioned, saline-treated), AD ($A\beta_{1-42}$-lesioned, saline-treated), GRg1 low dose ($A\beta_{1-42}$-lesioned, treated with GRg1 at 7.5 mg/kg/day), GRg1 moderate dose ($A\beta_{1-42}$-lesioned, treated with GRg1 at 15 mg/kg/day), GRg1 high dose ($A\beta_{1-42}$-lesioned, treated with GRg1 at 30 mg/kg/day), GRb1 low dose ($A\beta_{1-42}$-lesioned, treated with GRb1 at 7.5 mg/kg/day), GRb1 moderate dose ($A\beta_{1-42}$-lesioned, treated with GRb1 at 15 mg/kg/day), and GRb1 high dose ($A\beta_{1-42}$-lesioned, treated with GRb1 at 30 mg/kg/day).

Mice were anesthetized with chloral hydrate (200 mg/kg) and placed in a Kopf stereotaxis (David Kopf Instruments, Tujunga, CA, USA). Aggregated $A\beta_{1-42}$ peptide (3 μl) was then unilaterally injected into the hippocampal region (anterior-posterior, -2.00 mm; medial-lateral, 1.50 mm; dorsal-ventral, 1.0 mm) [19]. Mice in the control group were injected with saline. The $A\beta_{1-42}$ peptide was dissolved and diluted in saline to a concentration of 10 mg/ml and incubated at 37°C for 5 days to obtain the fibrillized form of the peptide before injection. GRg1 and GRb1 were delivered by intraperitoneal injection once daily for 1 month, while mice in the control and AD groups received 0.2 ml saline.

Morris water maze test

Spatial learning and memory were tested with the Morris water maze test with minor modifications [20]. A circular water tank (diameter × height, 120 × 40 cm) was filled with water at 23 ± 1°C and divided into four equal quadrants. A submerged platform (diameter × height, 8 × 10 cm) painted black was centered in the fourth quadrant 1 cm below the water surface. A camera placed 2 m above the center of the tank recorded escape latencies and path length during each trial. The Morris water maze test consisted of a place navigation test and a space exploration test. The place navigation test was performed two times per day for five consecutive days. The mice were trained to find and escape onto the platform. A different starting position for each mouse was used in each trial. For each individual mouse, the position of the platform was fixed during the entire experiment. The mice were allowed to swim freely to find the hidden platform within 60 s. Mice failed to find the location within the given time were gently guided to the platform and were allowed to stay on it for 10 s and then returned to the cage. The average escape latency, escape distance and swimming velocity of each mouse per day were calculated. On the day after the place navigation test, a spatial exploration test was conducted in which the platform was removed. The time spent swimming in the target quadrant (fourth) and the times crossing the platform location were measured for each mouse.

Sample collection and pretreatment

Mice were anesthetized with diethyl ether and brains were collected and weighed. 1.0 ml water was added to 0.1 g of brain tissue, and then the mixtures were homogenized in an ice bath. An aliquot of 600 μL of ice-cold methanol was then added to 150 μL aliquots of cerebral homogenate to precipitate protein, and the tubes was vortexed for 5 min followed by centrifugation at 13,000 rpm for 10 min at 4°C. The supernatant was transferred to another tube and evaporated to dryness at 30°C under a gentle stream of nitrogen. The dried residue was then reconstituted in 100 μL of acetonitrile-water (2:98, v/v) and 5 μL of this solution was injected into the UPLC-MS/MS system.

Spectrum acquisition

LC was performed on a Waters Acquity UPLC system (Waters Corp., Milford, MA, USA). Chromatographic separation was achieved on a Waters bridged ethyl hybrid C18 column (50 × 2.1 mm, 1.7 μm) maintained at 30°C. The auto-sampler was conditioned at 4°C and the injection volume was 5 ul. Gradient elution with a mobile phase composed of water and acetonitrile with 0.1% formic acid was performed as follows: 0 min 98% ~2%; 2 min 92% ~8%; 4 min 60% ~40% ; 12 min % ~88%; 18 min 0% ~100%; 21 min 2% ~98% at a flow rate of 0.25 ml/min (Table 1).

Mass spectrometric detection was carried out on a triple quadrupole tandem mass spectrometer with an electrospray ionization (ESI) interface. The ESI source was set in positive mode. The following parameters were used: capillary voltage, 3.2 kV; cone voltage, 30 V; source temperature, 120°C; and desolvation temperature, 350°C. Nitrogen was used for desolvation and as cone gas at flow rates of 600 and 50 l/h, respectively. Full scan mode was used in the mass range of 100-1000 amu. For MS/MS, argon was used as collision gas and collision energy was set according to metabolite composition. Data were collected in centroid mode. NaCsI was used for mass correction.

Data analysis

SPSS19 software was used to process the data of Morris water maze test parameters between groups by one-way analysis of variance (ANOVA) followed by Turkey multiple comparison tests. The results of the statistical analysis were expressed as mean ± standard deviation (mean ± SD). $P<0.05$ was considered to be significant difference for the test.

Raw data for sample were analyzed by Markerlynx within Masslynx software (version 4.1) for peak detection and alignment. The retention time and *m/z* data for each peak were determined by the software. All data were normalized to the summed total ion intensity per chromatogram. The main parameters of Markerlynx method were set as follows: The mass tolerance was set at 0.01 Da. The noise elimination level was set at 10.0. The initial and final retention time was set as 0 and 16 min, and the high and low mass were 100 and 1000 amu, respectively.

Group(nGroup (n=10)	Dose/mg.kg^{-1}	Escape latency/s					Time in the target quadrant/s	Platform crossing times
		1	2	3	4	5		
Normal	-	55.4 ± 11.2	40.0 ± 13.7	32.1 ± 7.1	24.6 ± 8.1	20.0 ± 8.0	24.2 ± 4.8	4.8 ± 1.3
Control	-	59.3 ± 1.9	42.4 ± 124	35.1 ± 9.7	28.3 ± 12.0	22.8 ± 5.6	23.9 ± 2.7	4.2 ± 1.3
AD	-	58.9 ± 3.2	53.3 ± 9.7	50.5 ± 11.0$^{\#}$	45.1 ± 12.2$^{\#}$	40.5 ± 9.3$^{\#\#\#}$	16.2 ± 3.0$^{\#\#\#}$	2.1 ± 0.8$^{\#}$
GRg1 L	7.5	58.7 ± 3.7	48.6 ± 9.4	45.8 ± 11.8	37.1 ± 10.4	31.9 ± 9.0	18.0 ± 3.0	3.2 ± 1.2
GRg1M	15.0	58.8 ± 3.5	46.6 ± 11.3	40.4 ± 9.3	33.4 ± 9.0	30.0 ± 7.0	18.9 ± 2.7	3.7 ± 1.6
GRg1 H	30.0	57.0 ± 9.2	46.6 ± 12.7	39.3 ± 9.8	30.1 ± 10.4*	26.2 ± 6.9**	21.7 ± 2.1**	4.0 ± 1.0*
GRb1 L	7.5	57.9 ± 6.4	49.0 ± 13.0	44.9 ± 11.9	38.6 ± 13.1	32.9 ± 7.8	18.8 ± 4.5	2.8 ± 1.0
GRb1M	15.0	56.9 ± 9.5	47.6 ± 12.4	42.0 ± 9.8	34.4 ± 9.0	29.8 ± 5.0	19.3 ± 2.1	3.6 ± 1.64
GRb1 H	30.0	55.9 ± 12.6	47.7 ± 11.4	41.3 ± 10.7	29.9 ± 4.6*	27.5 ± 8.2**	21.4 ± 3.3*	4.2 ± 1.0*

Table 1: Effects of GRg1and GRb1 on the performance of AD mice in the Morris water maze test.

Identification of endogenous metabolites

Samples were analyzed and low molecular weight metabolites were represented as the chromatographic peaks in the total ion chromatograms (TIC). The collision induced dissociation (CID) experiment was implemented to get fragmentation patterns of these potential biomarkers. Some biomarkers were identified by comparing their chromatographic retention time and MS/MS fragmentation characteristics with the available authentic references. Furthermore, full scan mass spectra of these metabolites were interpreted using available biochemical databases, such as Kyoto Encyclopedia of Genes and Genomes database (http://www.genome.jp/kegg), the Human Metabolome Database (http://www.hmdb.ca/) and so on. Meanwhile, some biomarkers were identified by the retention time and the accurate mass number of Bruker's ESI-QTOF-MS under the same liquid chromatography condition.

Results

GRg1 and GRb1 treatment improves Morris water maze test performance of AD mice

In the place navigation test, mice in the AD group took much more time to reach the platform on the last three training days compared to the control group ($P<0.05$). High doses of GRg1 or GRb1 reduced escape latency compared to the AD group on days 4 ($P<0.05$) and 5 ($P<0.01$) (Table 1). In the spatial exploration test, mice in the AD group spent less time in the target quadrant than those in the control group ($P<0.05$), a trend that was reversed by treatment with high doses of GRg1 or GRb1. Furthermore, the number of platform crossings was significantly decreased in the AD than in the control group ($P<0.05$); however, mice treated with high doses of GRg1 and GRb1 showed higher frequencies of platform crossings compared to the AD group ($P<0.05$). There was no difference in swimming speed across groups (data not shown). These results indicated that ginsenoside treatment ameliorates cognitive deficits in AD mice.

Metabolite profiles in AD

Method development and validation: Quantitative information was obtained in the positive rather than the negative ion mode. Molecular ions $[M+H]^+$ accounted for the majority of the mass spectrum. Extracted chromatographic peaks of seven ions were selected based on their chemical polarities and *m/z* values. The paired retention time *m/z* of these ions were as follows: 0.79 min_136.5,min 6.58_274.5, 6.64 min _318.5, 8.55 min _302.1,7.37 min _454.0, 10.1 min _496.5, 10.1 min _518.5, 10.1 min _544.5, 15.1 min _637.0, which were distributed in different regions of the spectrum and for which retention times were used for method validation. The relative standard deviations (RSDs) of peak intensities and retention times for selected ions in pooled brain tissue samples were calculated. Precision of injection was evaluated by the continuous detection of six replicates of the same sample. Precision RSDs were from 5.2% to 13.8% for peak intensity and from 0.8% to 2.4% for retention time. Six samples were prepared in parallel to minimize inter-sample variability. The method repeatability (RSD%) was 3.7%-14.0% for peak intensity and 0.8%-1.5% for retention time. The system stability, which was determined by injecting a quality control sample every five samples during the analysis, was 5.9%-10.0% for peak intensity and 0.9%-3.2% for retention time. The post-preparation stability of the sample was assessed by analyzing samples left in the autosampler at 4°C for 4, 8, 12, and 24 h. RSDs ranged from 2.9%-11.2% for peak intensity and 0.6%-2.5% for retention time. The precision, repeatability, and stability indicated that this was a robust method for analyzing brain tissue samples.

Metabolite profiling analysis: Representative positive ion TIC chromatograms of typical brain tissue samples from control and AD mice are shown in Figure 1. A pattern recognition approach using PCA, a non-supervised multivariate data analytical method, was used to reveal clustering trends in the data. In the PCA score, each point represented an individual sample; the plot of PCA scores divided different samples into blocks, suggesting different metabolic profiles. Samples from the control and AD groups were clearly divided into two classes (Figure 2a), indicating that the AD was successfully reproduced by this model and that specific biomarkers could distinguish AD from control mice. In the PCA loading plots for AD and control mice, the distance of an ion from the origin represents its influence on PCA components (Figure 2b).

Biomarker identification: Ions in the plot were selected as putative biomarkers (Table 2), and were those with retention time-*m/z* pairs of 0.79_136.5,6.58_274.5, 6.64_318.5, 8.55_302.1,7.37_454.0, 10.1_496.5, 10.1_518.5, 10.1_544.5, 15.1_637.0. Biomarkers at *m/z* 496.5, 518.5, 544.5 and were identified through comparisons to known retention times of standards and to the corresponding fragment from the product ion scan in positive mode. For instance, in the positive product ion scan for the biomarker at *m/z* 496 (Figure 3), the parent ion $[M+H]^+$ contained three major fragments; those at *m/z* 104 and 184.0 represented $[HOCH_2CH_2N(CH_3)_3]^+$ and $[H_2O_3PO–CH_2CH_2N(CH_3)_3]^+$, respectively, providing head group information for phosphatidylcholines (PCs). Another major fragment at *m/z* 478 $[M–H_2O+H]^+$ identified this marker as lyso PC C16:0. To evaluate changes in biomarker profiles, peak intensities of putative biomarkers of AD and control mice were compared (Figure 4). The peak intensities of lysophosphatidylcholine (LPC), and dihydrosphingosine were reduced and that of phenylalanine was elevated in the brain of AD as compared to control mice.

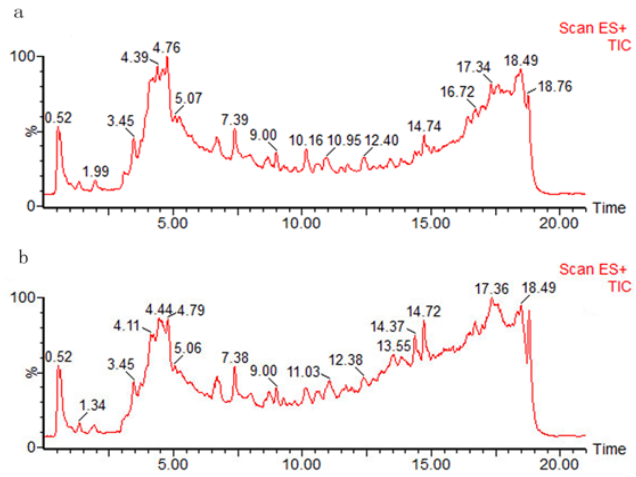

Figure 1: Typical positive TICs of representative brain tissue samples from (A) AD and (B) control animals.

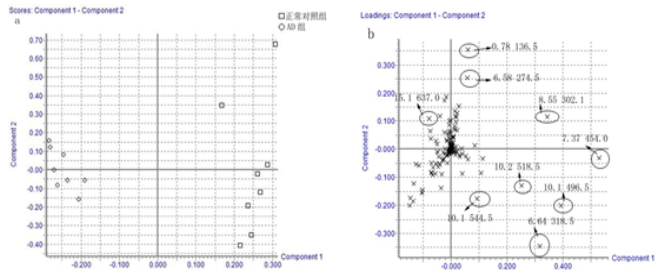

Figure 2: (A) Score and (B) loading plots from the PCA of control and AD mice.

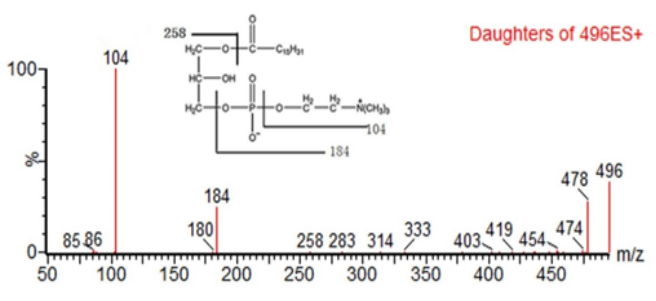

Figure 3: Product ion scan spectra of biomarkers in positive ion mode (*m/z* 496.5).

GRg1 and GRb1 treatment alters metabolite profiles of AD mice

According to the PCA score plots (Figure 5a) from processing dates of the control, AD, and GRg1- and GRb1-treated groups, samples from GRg1-treated groups were located in the middle of that from AD group and control group. The low dose group was located closely to AD group. In contrast, the high dose group was separated from the AD group and was closer to the controls, suggesting that GRg1 treatment partly restored metabolites in AD mice to normal levels. Metabolites with altered levels were identified in the PCA loading plot; the peak intensity of ceremide was decreased, while those of, dihydrosphingosine, hexadecasphinganine, phytosphingosine, LPC C18:3, C13:0, C20:4, C16:0) were increased in the GRg1 high dose as compared to the AD group ($P<0.05$) (Figure 6a).

Treatment with GRb1 obtained similar findings. The PCA plots of the low and moderate dose groups were located close to and showed some degree of overlaps with that of the AD group, while the plot for the high dose group was far removed from that of AD animals, and showed a trend to approach to that of controls (Figure 5b). The peak intensity of phenylalanine was decreased, while those of phytosphingosine and LPCs (LPC C18:3, C13:0, C20:4, C16:0) were increased by treatment with a high dose of GRb1 compared to the AD group ($P<0.05$) (Figure 6b). These results suggest that treatment with a high dose of GRg1 and GRb1 can protect the brain against metabolic alterations induced by $A\beta_{1-42}$.

Discussion

In this study, a UPLC-MS/MS-based metabolomics method was used to investigate the therapeutic effects of GRg1 and GRb1 on AD. The injection of $A\beta_{1-42}$ protein fragments into the ventricle, hippocampus, or other brain regions has been reported to have an ability to impair learning and memory [21-23]; In the Morris water maze test, mice treated with high doses of GRg1 and GRb1 showed superior performance to those in the AD group, indicating that ginsenosides can partly restore cognitive function in the AD model.

Hypoxanthine as the principal purine nucleobase involved in the brain's salvage purine pathway, belongs to purine compounds [24]. In purine pathway, it is generated to xanthine under the action of xanthine oxidase. In recent years, more and more studies have show that purine metabolic disorders are closely related to neurodegenerative diseases [25,26]. What's more, an increasing level was observed in the hippocampus of AD patients and the reason account for it might due to the loss of purine A1 receptor. In this study, compared with that in control group mice, the peak intensity of Hypoxanthine in AD model mice was significantly increased, which was in line with the previous reports. However, the level of Hypoxanthine was not significantly decreased with the treatment of GRg1 a GRb1. The above showed that Hypoxanthine can be a reliable biomarker for diagnosing AD, while the therapeutically effect of GRg1 a GRb1 did little to purine pathway.

In this study, the level of LPCs was obviously decreased in the brain tissue of AD mice compared to the control mice consistent with the previous reports that a lower total LPC concentration was observed in brain, CSF and plasma of AD patients [27-29]. LPC is the degradation product of Phosphatidylcholine (PC), which is the major phospholipid of eukaryotic membranes representing approximately 40% of phospholipids in most cellular membranes [30]. Thus the significantly decreased LPCs indicated that a disorder of lecithin metabolism appeared in AD mice. The principal function of phospholipids is maintaining the normal integrity of cell membranes [31]. Therefore, the disorder of lecithin metabolism could mean a lesion of cell membranes, which is reported to greatly related to AD [32]. A significant increase of LPCs was observed in our study with the treatment of GRg1 and GRb1. Therefore, we can hypothesize that GRg1 and GRb1 presented protective effect on AD through modulating the disorder of choline-containing phospholipids.

Dihydrosphingosine, hexadecasphinganine, phytosphingosine and ceremide are classified into sphingolipids. In our study, a decrease of dihydrosphingosine, hexadecasphinganine and phytosphingosine and a increase of ceremide in the brain of AD mice were observed compared with control mice, which is in accordance with the previous studies that there was a decrease of dihydrosphingosine in plasma of

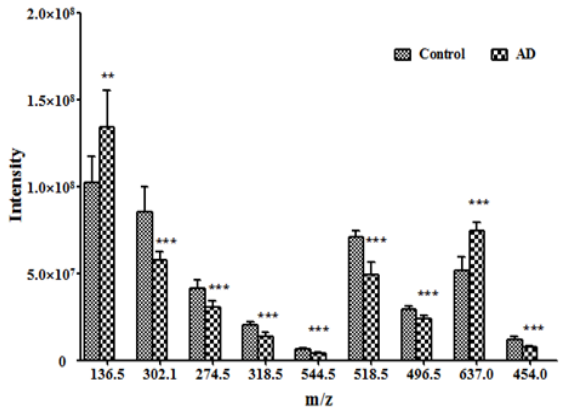

Figure 4: Peak intensity of potential biomarkers in the brain tissue of control and AD mice. Identification: 136.5 hypoxanthine; 274.5, Hexadecasphinganine; 318, Phytosphingosine; 302.1, dihydrosphingosine; 496.5, LPC C16:0; 520.5, LPC C18:2; 454.0, LPC C13:0; 518.5, LPC C18:3; 544.5, LPC C20:4; 637.0 ceremide 40:1. **P<0.01, ***P<0.001.

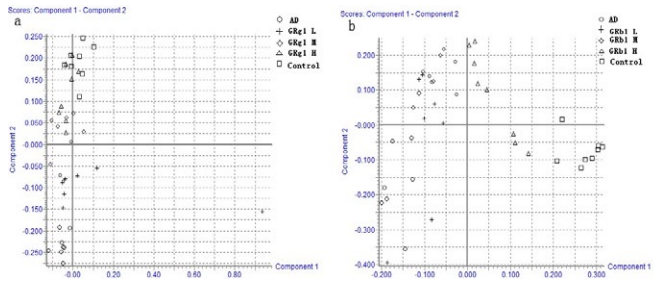

Figure 5: (a) Score plots from the PCA of AD and GRg1-treated mice. (b) Score plots from the PCA of AD and GRb1-treated mice.

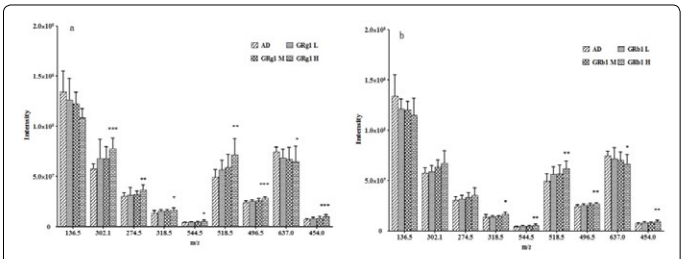

Figure 6: Peak intensity of potential biomarkers GRg1-treated mice (a) and GRb1-treated mice (b). Fragment identification is as described in the legend for Figure 4. *P<0.05, **P<0.01, ***P<0.001 vs. AD group.

Retention time	Z ratio	Scan mode	Excimer ion	Biomarkers	Trend (AD mice vs. Controls)
0.79	136.5	+	$[M+H]^+$	Hypoxanthine	↑
6.58	274.5	+	$[M+H]^+$	Hexadecasphinganine	↓
8.55	302.1	+	$[M+H]^+$	Dihydrosphingosine	↓
6.64	318.5	+	$[M+H]^+$	Phytosphingosine	↓
7.37	454.0	+	$[M+H]^+$	LPC C 13:0	↓
10.2	518.5	+	$[M+H]^+$	LPC C 18:3	↓
10.1	544.5	+	$[M+H]^+$	LPC C 20:4	↓
10.1	496.5	+	$[M+H]^+$	LPC C 16:0	↓
15.1	637.0	+	$[M+H]^+$	Ceramide 40:1	↑

Table 2: Potential biomarkers identified in AD and control mice by ultra-performance liquid chromatography-mass spectrometry.

AD patient [29] and the level of ceramides was significantly increased in the plasma, serum and brain of AD patients [33-35]. Central nervous system contains large amounts of sphingolipids ; Their metabolites have important structural roles in cell membranes and function as second messengers for critical intra- and inter-cellular signaling affecting cellular growth, differentiation, proliferation, and apoptosis [36]. At high levels, Ceramides inhibit cell division, promote stress signaling cascades and induce apoptosis [37]. Ceramides are also intermediates linking inflammatory cytokines to insulin resistance and subclinical atherosclerosis, all of which are associated with an increased risk of AD [38-40]. These observations indicate that dihydrosphingosine, hexadecasphinganine, phytosphingosine and ceremide can be reliable biomarkers for diagnosing AD. The reasons underlying for it are not clear, but some studies have shown that dysregulation of sphingolipid metabolism results from a reduction in sphingosine kinase-1 and increase in sphingosine 1-phosphate lyase activities [41,42]. The treatment of high dose of GRg1 and GRb1 can partly restore the disorder of sphingolipids metabolim with little difference that the level of dihydrosphingosine, hexadecasphinganine, phytosphingosine and ceremide was significantly altered in high-dose of GRg1 treated mice,while there was no significant change in the level of dihydrosphingosine, hexadecasphinganine in the GRb1 treated groups. The reason account for It was possibly due to their different chemical structures that GRg1 is protopanaxatriol with two sugars, while GRb1 is protopanaxadiol with four sugars [43].

Conclusion

In this study, a UPLC-MS based metabolomics approach was used to investigate changes in metabolite levels in the brain of AD mice following GRg1 and GRb1 treatment. A total of 9 metabolites including LPCs, hypoxanthine, dihydrosphingosine hexadecasphinganine, phytosphingosine and ceremide were identified in AD mice that are potential biomarkers for measuring the protective effects of GRg1 and GRb1, which likely regulate lecithin, and/or sphingolipid metabolism. These findings provide molecular evidence for the efficacy of ginsenosides as agents for the treatment of AD.

Acknowledgements

The authors thank Yingge Gong for technical assistance. The study was supported by the National Natural Science Foundation of China (No. 81203002) and the Shenyang Science and Technology Program (No. F12-193-9-22).

References

1. Selkoe DJ (2001) Alzheimer's disease: genes, proteins, and therapy. Physiological reviews 81: 741-766.
2. Praticò D (2008) Oxidative stress hypothesis in Alzheimer's disease: a reappraisal. Trends in pharmacological sciences 29: 609-615.
3. Kim HJ, Kim P, CY S (2013) A comprehensive review of the therapeutic and pharmacological effects of ginseng and ginsenosides in central nervous system. Journal of Ginseng Research 37: 8-29.
4. Ik-Hyun Cho (2012) Effects of Panax ginseng in Neurodegenerative Diseases. Journal of Ginseng Research 36: 342-353.
5. Xie X, Wang HT, Li CL, Gao XH, Ding JL, *et al*. (2010) Ginsenoside Rb1 protects PC12 cells against β-amyloid-induced cell injury. Molecular medicine reports 3: 635-639.
6. LH Tu, Ma J, Liu HP, Wang RR, Luo J (2009) The neuroprotective effects of ginsenosides on calcineurin activity and tau phosphorylation in SY5Y cells. Cellular and molecular neurobiology 29: 1257-1264.
7. Nishiyama N, Cho SI, Kitagawa I, Saito H (1994) Malonylginsenoside Rb1 potentiates nerve growth factor (NGF)-induced neurite outgrowth of cultured chick embryonic dorsal root ganglia. Biol Pharm Bull 17: 509-513.

8. Wu CF, Bi XL, Yang JY, Zhan JY, Dong YX, *et al.* (2007) Differential effects of ginsenosides on NO and TNF-alpha production by LPS-activated N9 microglia. Int Immunopharmacol 7: 313-320.

9. Chen F, Eckman EA, Eckman CB (2006) Reductions in levels of the Alzheimer's amyloid beta peptide after oral administration of ginsenosides. FASEB J 20: 1269-1271.

10. Lindon JC, Holmes E, Nicholson JK (2004) Metabolomics and its role in drug development and disease diagnosis. Expert Review of Molecular Diagnostics 4: 189-199.

11. Ibáñez C, Simó C, Cifuentes A (2013) Metabolomics in Alzheimer's disease research. Electrophoresis 34: 2799-2811.

12. Graham SF, Chevallier OP, Roberts D, Hölscher C, Elliott CT (2013) Investigation of the human brain metabolome to identify potential markers for early diagnosis and therapeutic targets of Alzheimer's disease. Analytical chemistry 85: 1803-1811.

13. Botosoa E, Zhu M, Marbeuf-Gueye C, Triba M, Dutheil F, *et al.* (2012) NMR metabolomic of frontal cortex extracts: First study comparing two neurodegenerative diseases Alzheimer disease and amyotrophic lateral sclerosis. IRBM 33: 281-286.

14. Inoue K, Tsutsui H, Akatsu H, Hashizume Y, Matsukawa N, *et al.* (2013) Metabolic profiling of Alzheimer's disease brains. Scientific Reports 3: 1-9.

15. Neha, Sodhi RK, Jaggi AS, Singh N (2014) Animal models of dementia and cognitive dysfunction. Life Sciences 109: 73-86.

16. Lu P, Mamiya T, Lu L, Mouri A, Zou L, *et al.* (2009) Silibinin prevents amyloid beta peptide-induced memory impairment and oxidative stress in mice. British Journal of Pharmacology 157: 1270-1277.

17. Li X, Zhao X, Xu X, Mao Xin, Liu Z, *et al.* (2014) Schisantherin A recovers Aβ-induced neurodegeneration with cognitive decline in mice. Physiology & Behavior 132: 10-16.

18. Shen WX, Chen JH, Jian-Hua Lu, Peng YP, Qiu YH (2014) TGF-β1 Protection against Aβ1-42-Induced Neuroinflammation and Neurodegeneration in Rats. International Journal of Molecular Sciences 15: 22092-22108.

19. Lee HE, Kim DH, Park SJ, Kim JM, Lee YW, *et al.* (2012) Neuroprotective effect of sinapic acid in a mouse model of amyloid β1-42 protein-induced Alzheimer's disease. Pharmacology Biochemistry and Behavior 103: 260-266.

20. Morris R (1984) Developments of a water-maze procedure for studying spatial learning in the rat. Journal of neuroscience methods 11: 47-60.

21. Choi JG, Moon M, Kim HG, Mook-Jung I, Chung SY, *et al.* (2011) Gami-Chunghyuldan ameliorates memory impairment and neurodegeneration induced by intrahippocampal Aβ1-42 oligomer injection. Neurobiology of learning and memory 96: 306-314.

22. Brouillette J, Caillierez R, Zommer N, Alves-Pires C, Benilova I, *et al.* (2012) Neurotoxicity and memory deficits induced by soluble low-molecular-weight amyloid-β1-42 oligomers are revealed in vivo by using a novel animal model. The Journal of Neuroscience 32: 7852-7861.

23. Liu RY, Gu R, Qi XL, Zhang T, Zhao Y, *et al.* (2008) Decreased nicotinic receptors and cognitive deficit in rats intracerebroventricularly injected with beta□amyloid peptide (1‐42) and fed a high‐cholesterol diet. Journal of neuroscience research 86: 183-193.

24. Bavaresco CS, Chiarani F, Matte C, Wajner M, Netto CA (2005) Effect of hypoxanthine on Na+, K+-ATPase activity and some parameters of oxidative stress in rat striatum. Brain Res 1041: 198-204.

25. Kaddurah-Daouk R, Rozen S, Matson W, Han X, Hulette CM, *et al.* (2011) Metabolomic changes in autopsy-confirmed Alzheimer's disease. Alzheimer's & Dementia 7: 309-317.

26. Kaddurah-Daouk R, Zhu H, Sharma S, Bogdanov M, Rozen S, *et al.* (2013) Alterations in metabolic pathways and networks in Alzheimer's disease. Translational psychiatry 3: 1-8.

27. Mulder C, Wahlund LO, Teerlink T, Blomberg M, Veerhuis R (2003) Decreased Lysophosphatidylcholine/phosphatidylcholine ratio in cerebrospinal fluid in Alzheimer's disease. Journal of neural transmission 110: 949-955.

28. Grimm MO, Grösgen S, Riemenschneider M, Tanila H, Grimm HS, *et al.* (2011) From brain to food: Analysis of phosphatidylcholins, lyso-phosphatidylcholins and phosphatidylcholin-plasmalogens derivates in Alzheimer's disease human post mortem brains and mice model via mass spectrometry. Journal of Chromatography A 1218: 7713-7722.

29. Nai-jing Li, Wen-tao Liu, Wei Li, Sheng-qi Li, Xiao-hui Chen, *et al.* (2010) Plasma metabolic profiling of Alzheimer's disease by liquid chromatography/mass spectrometry. Clinical biochemistry 43: 992-997.

30. Klein J (2000) Membrane breakdown in acute and chronic neurodegeneration: focus on choline-containing phospholipids. Journal of neural transmission 107: 1027-1063.

31. Vance DE (2014) Phospholipid methylation in mammals: from biochemistry to physiological function. Biochimica et Biophysica Acta (BBA)-Biomembranes 1838: 1477-1487.

32. Vestergaard MdC, Morita M, Hamada T, Takagi M, (2013) Membrane fusion and vesicular transformation induced by Alzheimer's amyloid beta. Biochimica et Biophysica Acta (BBA)-Biomembranes 1828: 1314-1321.

33. Mielke MM, Bandaru VVR, Haughey NJ, Rabins PV, Lyketsos CG, *et al.* (2010) Serum sphingomyelins and ceramides are early predictors of memory impairment. Neurobiology of aging 31: 17-24.

34. Mielke MM, Haughey NJ, Bandaru VVR, Weinberg DD, Darby E, *et al.* (2011) Plasma sphingomyelins are associated with cognitive progression in Alzheimer's disease. Journal of Alzheimer's Disease 27: 259-269.

35. Haughey NJ, Bandaru VV, Bae M, Mattson MP (2010) Roles for dysfunctional sphingolipid metabolism in Alzheimer's disease neuropathogenesis. Biochimica et Biophysica Acta (BBA)-Molecular and Cell Biology of Lipids 1801: 878-886.

36. Alessenko AV (2013) The potential role for sphingolipids in neuropathogenesis of Alzheimer's disease. Biochemistry (Moscow) Supplement Series B: Biomedical Chemistry 7: 108-123.

37. Bruce AJ, Boling W, Kindy MS (1996) Altered neuronal and microglial responses to excitotoxic and ischemic brain injury in mice lacking TNF receptors. Nature medicine 2: 788-794.

38. Summers SA (2006) Ceramides in insulin resistance and lipotoxicity. Progress in lipid research 45: 42-72.

39. Ichi I, Nakahara K, Miyashita Y, Hidaka A, Kutsukake S, *et al.* (2006) Association of ceramides in human plasma with risk factors of atherosclerosis. Lipids 41: 859-863.

40. Nelson JC, Jiang XC, Tabas I, Tall A, Shea S (2006) Plasma sphingomyelin and subclinical atherosclerosis: findings from the multi-ethnic study of atherosclerosis. American journal of epidemiology 163: 903-912.

41. He X, Huang Y, Li B, Gong CX, Schuchman EH (2010) Deregulation of sphingolipid metabolism in Alzheimer's disease. Neurobiology of aging 31: 398-408.

42. Ceccom J, Loukh N, Lauwers-Cances V, Touriol C, Nicaise Y (2014) Reduced sphingosine kinase-1 and enhanced sphingosine 1-phosphate lyase expression demonstrate deregulated sphingosine 1-phosphate signaling in Alzheimer's disease. Acta Neuropathologica Communications 2: 1-10.

43. Cheng Y, Shen LH, Zhang JT (2005) Anti‐amnestic and anti‐aging effects of ginsenoside Rg1 and Rb1 and its mechanism of action. ACTA pharmacologica sinica 26: 143-149.